Analytical and Experimental Vibration and Buckling Characteristics of a Pretensioned Stayed Column

W. Keith Belvin*
NASA Langley Research Center, Hampton, Virginia

Modal vibration tests to determine the lateral modes of vibration of a stayed column and static axial compression tests to determine the column's buckling and postbuckling behavior have been performed. Effects of stay tension levels and vibration-load interaction are presented. Two finite element models are used to analyze the column, a three-dimensional frame using NASTRAN, and an equivalent two-dimensional frame using an exact dynamic stiffness matrix. Both analyses correlated well with the linear vibration and buckling experimental data. Results indicate premature buckling of the column due to vibration-load interaction and nonlinear oscillations due to stay slackening. Postbuckling behavior of the column is unusual because of stay slackening and results in a post-buckling restoring force of less than the bifurcation buckling load. Guidelines for design of pretensioned structures are presented which consider buckling, postbuckling, and vibration behavior.

Nomenclature

A_s = cross-sectional area of stay
D_n = length of nth stay
E_c = Young's modulus of central tube material
E_s = Young's modulus of stay material
f = frequency, Hz
I_c = area moment of inertia of central tube
I_s = area moment of inertia of stay
K_n = equivalent lateral stiffness provided to central tube by nth stay set
L = length of central tube
l = bay length, L/N
M = number of stay planes
N = number of bays (8 for the stayed column tested)
n = integer representing stay set from center to end, 1, 2, 3, 4, respectively
P = axial compressive load
P_{cr} = bifurcation buckling load
R = radius of stayed column and spoke length
S = integer representing Sth lateral cable mode, $S = 1, 2, 3 \ldots$
T = tensile force
T_n = tension in nth stay
ρ = mass per unit length of stay
ϵ = fabrication imperfection 1.16×10^{-4} (m/m), (Ref. 5)
λ = ratio between applied load and general instability load, = 0.417 (Ref. 5)
ω = modal frequency with external compressive load
ω_0 = initial modal frequency with no external load

Introduction

SEVERAL types of structures are being considered for space applications with objectives of low mass, deployability, and dense packaged volume to achieve efficient transportation to Earth orbit. Most structures possess only one or two of these qualities. However, pretensioned structures have the potential of fulfilling all three needs. Pretensioned structures use tension elements to provide lateral stiffness and stability to compression members. Conceptually pretensioned members could be used to stiffen an entire structure such as the hoop-column antenna[1] (see Fig. 1) or to form erectable elements of a larger structure. For example, pretensioned stayed columns could be used as elements of truss type platforms.

Stayed columns have been shown to be very efficient when the dimensionless index P/E_cL^2 is small.[2] Current uses of stayed columns are found in offshore structures and ship masts. The use of stayed columns in space is a natural extension. Loads generated in large space structures usually result from accelerations produced by orbital transfer, docking, and attitude control.[3] Thus, member loads often result solely from the inertial forces induced by the mass of the structure. Minimum mass structures not only enable efficient transportation to Earth orbit, but also minimize the on-orbit member loads. The low mass of pretensioned structures satisfies the condition of small P/E_cL^2 when used in space.

This paper reports the results of an experimental and analytical investigation of the vibration and buckling characteristics of a fundamental pretensioned structure, the stayed column. Analysis and experiments were performed to examine the effects of vibration-load interaction, initial imperfections, and stay tension levels. Analysis was carried out using two linear finite element models. Experiments consisted of measuring vibration mode shapes and natural frequencies with and without compressive end load. In addition, static buckling

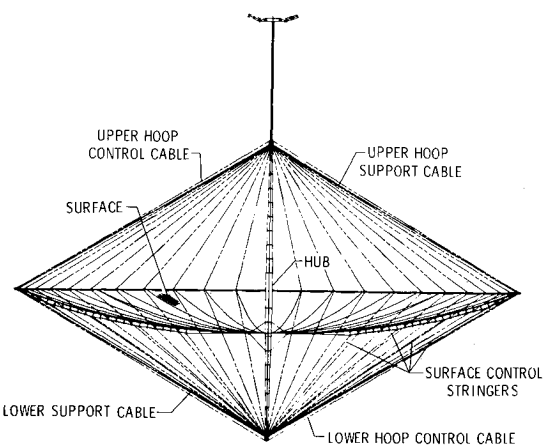

Fig. 1 Cable-stiffened hoop-column antenna.

Presented as Paper 82-0775 at the AIAA/ASME/ASLE/AHS 23rd Structures, Structural Dynamics and Materials Conference, New Orleans, La., May 10-12, 1982; received July 12, 1982; revision received Oct. 24, 1983. This paper is declared a work of the U.S. Government and therefore is in the public domain.

*Aerospace Technologist, Structures & Dynamics Division, Structural Dynamics Branch. Member AIAA.

tests were performed to ascertain prebuckling and postbuckling behavior. Experimental data is used to show the limits of linear analysis and several unusual characteristics of pretensioned structures.

Column Description

The test article, shown in Fig. 2 and schematically in Fig. 3, uses 24 pretensioned elements, called stays, to provide lateral stability to the main compression member, hereafter referred to as the central tube. The stays are made of 1.02 mm diameter graphite epoxy material and the central tube consists of an aluminum thin wall tube 5.2 m in length, and 9.53 mm in outer diameter with a wall thickness of 0.71 mm. Compression due to both external compressive loads and stay tension reactive loads exists in the central tube. Three graphite epoxy radial spokes, 3.89 mm in diameter, are used to offset the stays from the central tube. The spokes carry compression induced by stay tension. Three battens, fabricated from the stay material, are used to position the spoke ends at 120-deg intervals around the central tube. Seven constant force spring capsules, shown schematically in Fig. 4, are used to pretension the stays. (One end stay set is rigidly attached to the central tube.) Each spring capsule produces a constant force directed along the central tube axes. The measured spring capsule forces are 5.1, 5.1, 14.7, and 30.9 N applied to the $n = 1, 2, 3,$ and 4 stay sets, respectively.[4] The mass of individual parts and fabrication drawings are presented in Ref. 4.

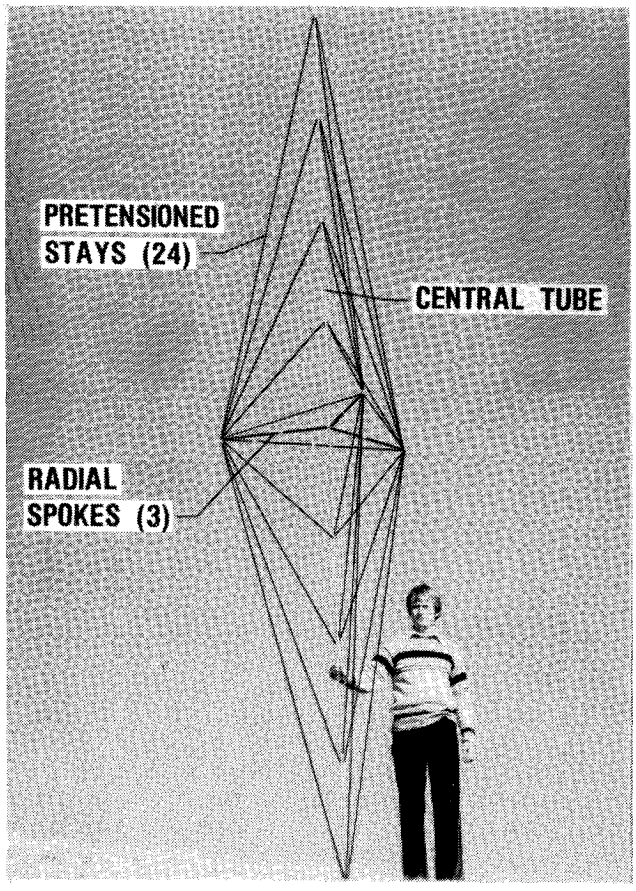

Fig. 2 Photograph of stayed column.

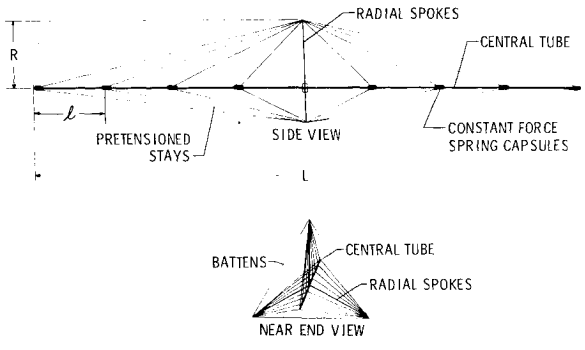

Fig. 3 Elements of stayed column.

Design Rationale

The principle of a stayed column is to increase the lateral stiffness of the central tube by pretensioned stays. Most stayed column designs are based on static stability and the present design is no exception. However, this design is unusual in that imperfection analysis was used to size the stay tension levels. Since Hedgepeth[5] gives a complete description of the design of this column, only a brief description will be given here.

The Euler buckling load of a pinned-pinned prismatic column of length L, given by the equation

$$P_{cr} = \pi^2 E_c I_c / L^2 \tag{1}$$

may be increased by increasing Young's modulus, increasing the area moment of inertia, or by reducing the effective length of the column. The stayed column concept reduces the effective length by providing intermediate elastic supports. Figure 5 shows a simple mathematical representation used to design static stability. If the springs K_n are such that

$$K_n \geq 4P/l \tag{2}$$

then buckling occurs between bays.[6] Thus, the effective length of the central tube is L/N. Substituting the effective length into Eq. (1) increases the Euler load by the factor N^2. A simple expression for K_n may be obtained by assuming the spokes have infinite extensional stiffness. Then

$$K_n = \tfrac{3}{2} E_s A_s R^2 / D_n^3 \tag{3}$$

The necessary stay stiffness for a design load P and bay length l may be obtained by equating Eqs. (2) and (3).

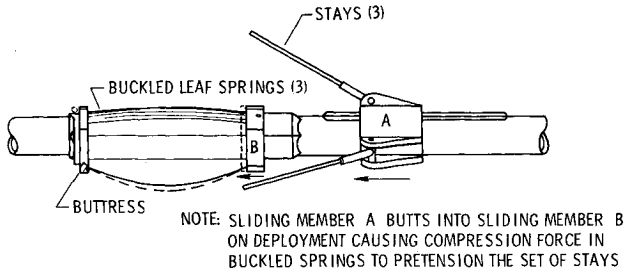

Fig. 4 Constant force spring capsule.

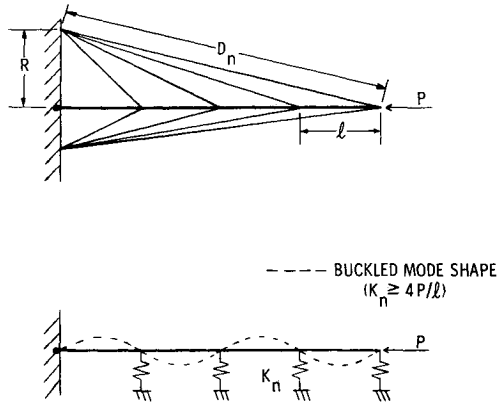

Fig. 5 Stay stiffness contribution to half-model.

To produce the stiffness given by Eq. (3), the stays must remain taut. The column was designed assuming fabrication tolerances would create imperfections in stay length. Errors in stay length produce initial curvature in the central tube. Since axial compression produces lateral forces in an initially curved column, the stay tension level was designed to prevent stay slackening in the presence of these lateral forces.

The geometry of the column was chosen to obtain high structural efficiency. The total mass of the stayed column was developed in algebraic form as a function of the number of bays, the spoke length to column length ratio, and other variables by Hedgepeth.[5] The mass of the column was minimized by assessing the effects of various parameters. Eight bays and a spoke length to column length ratio of 0.125 were found to yield high structural efficiency. The column was also designed to be deployable. Sliding stay attachments and spoke hinges were used to allow the column to be packaged. Deployment is accomplished by moving the radial spokes outward from the column. When packaged, the column maintains the original length; however, the diameter reduces to approximately twice the diameter of the central tube.

Instrumentation and Test Procedure

The column was mounted vertically in a loading fixture as shown schematically in Fig. 6. Simple supports were obtained with the use of ball joints mounted at each end of the column. A counterbalance was used to cancel weight effects of the lever arm and load pan. The axial load applied to the column was equal to twice the pan load due to the geometry of the loading fixture.

Buckling

The column was loaded and end shortening was measured with a noncontacting proximity probe, also shown in Fig. 6. All shortening measurements were made assuming the ball joints and the floor were rigid. The column was buckled three times to assess repeatability of the measurements.

Vibration

The vibration characteristics of the column were obtained by exciting the central tube with lateral forces. Sinusoidal excitation was provided by a 4.45 N electrodynamic shaker. A servo controller and oscillator were used to maintain a constant sinusoidal exciter force. The response of the central tube with and without axial loading was measured by 15 noncontacting proximity probes, mounted as shown in Fig. 6, as the exciter force was swept in frequency from 10 to 60 Hz. A co-quad analyzer was used to determine the quadrature component of the displacement (90 deg out of phase with the input force). Resonant frequencies were obtained by analyzing the frequencies of peak quadrature response. Mode shapes were determined by analyzing the response of all probes at a given resonant frequency.

Since only structural modes that were dominated by central tube displacements were desired, the stays, battens, and spokes were not instrumented. However, the first resonant frequency of each stay was measured with a strobe light during free decay.

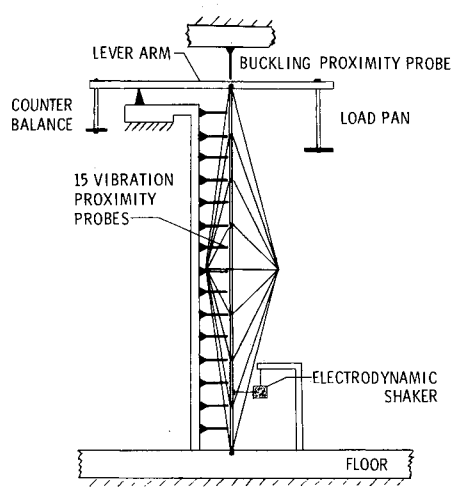

Fig. 6 Schematic diagram of test apparatus.

Analytical Models

The column was modeled as a three-dimensional frame using the NASTRAN finite element program. Each stay was modeled as a single bar element, since only those modes dominated by central tube deflections were desired. Each bay of the central tube was modeled with four bar elements. The sliding degree of freedom between the stays and the central tube was modeled by use of multipoint constraints. The pretension forces on the stays and the precompression on the central tube were included by a geometric stiffness matrix.

A second model used the theory of Williams and Howson to reduce the three-dimensional frame to a two-dimensional frame.[7,8] For example, the end view of the column shown in Fig. 7 may be reduced to an approximate planar column. This is accomplished by multiplying the areas, internal forces, and moments of inertia of the stays and spokes by $M/2$ or $3/2$ for the column shown. The central tube is constrained to deflect in the plane of the stays. For dynamic analyses, the additional mass of the spokes and stays must be lumped on the central tube. Also, this transformation requires the battens to be neglected.

After reducing the column to a planar frame, a finite element program called VIPASA was used to model the column.[9,10] Since VIPASA is programmed with exact elements (i.e., dynamic stiffness), only one element was required to model each stay and similarly one element for each bay of the central tube. In addition, VIPASA permits a very general method of incorporating both variable and constant member loads. The reduced number of elements required in the two-dimensional analyses substantially reduced computation costs.

Results and Discussion

Buckling

The buckled mode shape and the measured and predicted buckling loads from both analyses are shown in Fig. 8. Both analyses agree within 2% of the observed buckling load of 277.4 N. Since the initial precompression (55.8 N) is highest in the center bays, they exhibit the larger deflections. Anticipating this, a conservative buckling analysis of the column was performed in Ref. 5 by assuming that the buckling load of the stayed column would be the Euler load of the center bay minus the precompression in that bay. This resulted in a

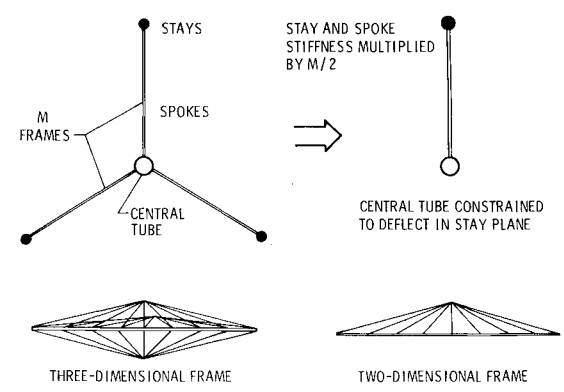

Fig. 7 Approximate two-dimensional model.

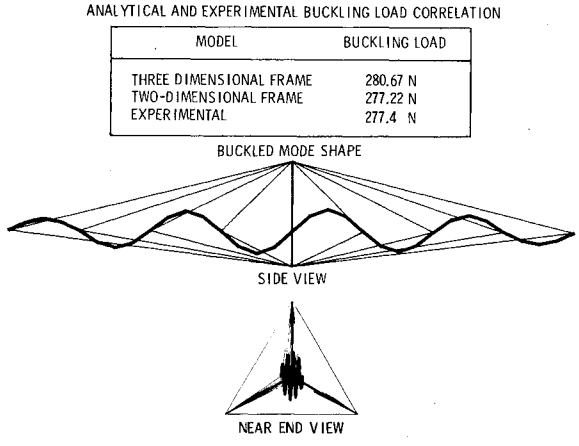

Fig. 8 Results of linear buckling analysis and experiment.

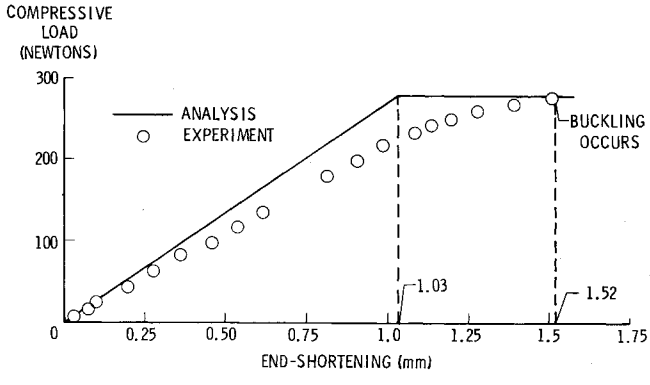

Fig. 9 Load end shortening correlation.

buckling load of 263.4 N, which is conservative by only 5% and thus useful in design calculations.

The measured and predicted load-end shortening curves for the column are shown in Fig. 9. The predicted end shortening assumes no initial imperfections and the deviation between the measured and predicted curves is attributed to initial curvature of the central tube. The stress at buckling in the central tube and stays is less than 10% of yield; consequently, no inelastic behavior occurred.

Postbuckling

At buckling, the column exhibits unusual behavior. The end shortening that occurs after buckling results in slackening of the stays. Some stays slacken while others remain taut, depending on imperfection effects. When the stays become slack, they no longer provide the lateral stiffness required to form nodes in the central tube. Thus the central tube buckles into a mode associated with a lower load. If the bifurcation load remains on the column, end shortening continues to slacken stays and an overall bending mode occurs. The postbuckling restoring force can be illustrated by the equilibrium path of Fig. 10. At buckling, a restoring force equal to the initial buckling load is exhibited until end shortening causes stay slackening. The restoring force with some stays slack depends on the degree of end shortening as well as imperfections. When all stays are slack, an overall bending mode occurs and the restoring force reduces to the unstiffened central tube buckling load of 5.0 N.

When the external load is removed after buckling, the column may not restore to the original shape due to precompression of the central tube by the stays. If an overall bending mode occurs, the stay-induced compressive load must be below the overall slack stay buckling load of 5.0 N to return to the original shape. Otherwise, the postbuckling equilibrium position will persist and the stayed column will not return to

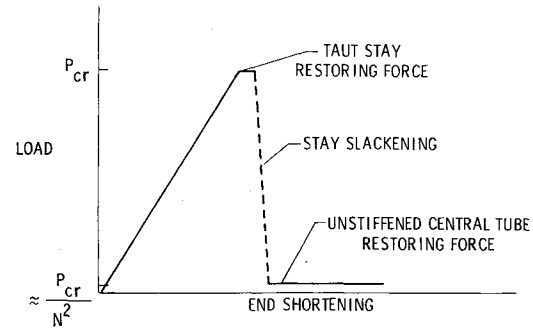

Fig. 10 Postbuckling equilibrium path.

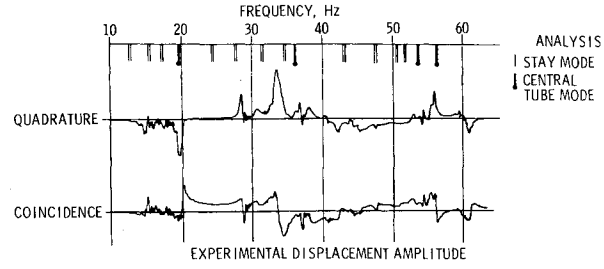

Fig. 11 Frequency spectrum from 10 to 60 Hz.

Table 1 Measured stay frequencies ($S = 1$)

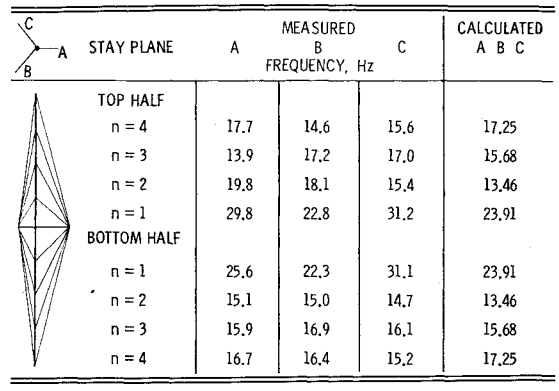

STAY PLANE	MEASURED FREQUENCY, Hz A	B	C	CALCULATED A B C
TOP HALF				
n = 4	17.7	14.6	15.6	17.25
n = 3	13.9	17.2	17.0	15.68
n = 2	19.8	18.1	15.4	13.46
n = 1	29.8	22.8	31.2	23.91
BOTTOM HALF				
n = 1	25.6	22.3	31.1	23.91
n = 2	15.1	15.0	14.7	13.46
n = 3	15.9	16.9	16.1	15.68
n = 4	16.7	16.4	15.2	17.25

the original shape unless redeployed. This behavior may indicate a guideline for design engineers. A safe margin between design load and buckling load must be designed to preclude catastrophic failure resulting from an instantaneous buckled state.

Vibrational Response

Response of the column to dynamic excitation is difficult to analyze due to the large number of natural frequencies of the structure (i.e., high modal density). The stays have lateral resonances near the first central tube bending modes. Since there are eight sets of stays, the response of the structure has high modal density. Figure 11 shows typical quadrature and coincidence components of the displacement from 10 to 60 Hz. The first central tube vibration mode occurs at 19.9 Hz. The large number of peaks in the response prior to this frequency represent stay resonances. Figure 11 also shows two-dimensional analytically predicted stay and central tube frequencies. Analysis predicts only three pairs of stay modes (symmetric and antisymmetric) below 19.9 Hz. The large number of experimental stay modes is a result of stay length imperfections which induce different tension levels in individual stays. Although the total tension in a set of stays is controlled during fabrication, this load may not be equally divided among the stays. Thus, each stay may have a different resonant frequency as shown by the measured stay frequencies in Table 1. The high modal density of lateral stay modes

produces coupling with vibration modes dominated by central tube deflections which could make active control of central tube modes difficult.

The column exhibited nonlinear behavior during most of the vibration tests. The resonant frequencies of the column changed with input force level and shaker location (i.e., mass effects) and with time. Nevertheless, the resonant frequencies reported are believed to represent the linear response of the column. Understanding the nonlinear characteristics of this column would require more control over stay tension levels and member imperfections than is attainable with this model. Consequently, observations of nonlinear behavior were only qualitative.

Modes with No Compressive Load

As in the case of buckling, the vibration modes dominated by central tube deflections have been analyzed by two methods. Correlation between analysis and test data with no compressive load is shown in Fig. 12. Both analyses predict the first mode within 2.3% of the experimental frequency (19.9 Hz). The first mode shape of the central tube is an overall bending mode; however, the elastic support provided by the stays restrains the deflection of the central tube from being sinusoidal. The stiffness in this mode is due mainly to the lateral stiffness provided by the exterior stays ($n = 4$). By doubling the diameter of these stays in the analysis, the frequency of the first mode increased 69.4% to 33.26 Hz. Thus a change in the exterior stay stiffness can be used to shift the frequency of the first central tube mode significantly.

A second bending mode of the central tube occurs at 34.1 Hz. The greater part of central tube bending occurs in the $n = 3$ and $n = 4$ bays. Two-dimensional analysis predicts a 5.8% higher frequency than observed experimentally. This mode is rotational in nature and is restrained by the rotational stiffness provided by the exterior stays. By doubling the exterior stay diameter an increase in the second bending frequency of 34.3% to 48.42 Hz is calculated.

The third vibration mode of the central tube is bending between bays, and is the same mode shape as initial buckling. Approximately 4.0% difference exists between the observed frequency of 56.5 Hz and the predicted frequencies of 54.21 and 54.64 Hz obtained from the two analyses. Both analyses assume the stays intersect the central tube centerline and that the entire bay length has the stiffness properties of the central tube. Actually, the constant force spring capsules offset the stays from the central tube and provide some bending stiffness to the central tube over the spring capsule length. This additional stiffness is believed to cause the higher experimental frequency. Unlike the first two modes, the mode primarily involving bending between bays would occur at the same frequency regardless of stay stiffness.

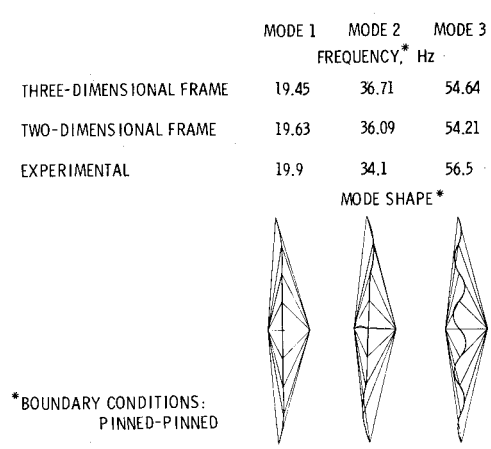

Fig. 12 Central tube vibration mode shapes and frequencies.

Effect of Compressive End Load

Figure 13 shows the effect of compressive end load on the first three central tube natural frequencies. Analysis predicts that the frequency of the first and second modes would not be strongly affected by the addition of compressive load. However, the third vibration mode, which has the same shape as the buckling mode, is reduced in frequency by the approximate equation

$$\omega^2 = \omega_0^2(1 - P/P_{cr}) \tag{4}$$

Equation (4) is valid, provided the vibration mode shape does not change with axial load P. In general, Eq. (4) predicts the reduction in frequency well for all modes. The first and second modes exhibit little reduction in the range shown, since the buckling loads associated with these mode shapes are very high.

Near a load of 162. N the third mode starts to deviate from the frequency predicted by Eq. (4). Since both the third mode and the second mode are antisymmetric they become coupled, i.e., each of the modes takes on characteristics of the second and third uncoupled modes. The analyses showed that the third mode shape slowly transforms into the second bending mode, and, similarly, the second mode shape transforms into bending between bays. Since the first mode is symmetric, no coupling exists between the mode involving bending between bays and the first bending mode.

To verify the frequency reduction predicted by analysis, modal tests with various compressive loads were performed. Experiments used a sinusoidal excitation force of 0.089 N. When a compressive load is applied to the column, the lateral deflections created by the exciter force are amplified. At load levels below 50% of the buckling load, experimental data were easily acquired. Figure 13 shows several experimental data points which verify that the frequency of the first two central tube modes were not significantly affected by the compressive load. Above 50% of the buckling load, the lateral deflections were amplified until isolated stay slackening occurred. Since slack stays do not contribute lateral stiffness to the central tube, nonlinear deflections resulted. When the input force was reduced to 0.0089 N, nonlinear deflections continued to occur. Smaller excitation levels were not practical with available equipment; consequently, verification of coupling between third and second modes was not obtained experimentally.

The implication for design is that in a dynamic environment, vibration load interaction may produce premature collapse of the column due to stay slackening. In Ref. 5, the design tension level is based on imperfections due to fabrication tolerances. Based on these results, the design engineer should consider both fabrication tolerances and vibration induced deflections in sizing stay tension levels.

Stay Tension Effects

To increase the linear deflection range of the central tube, stay tension must be increased. Parametric studies were per-

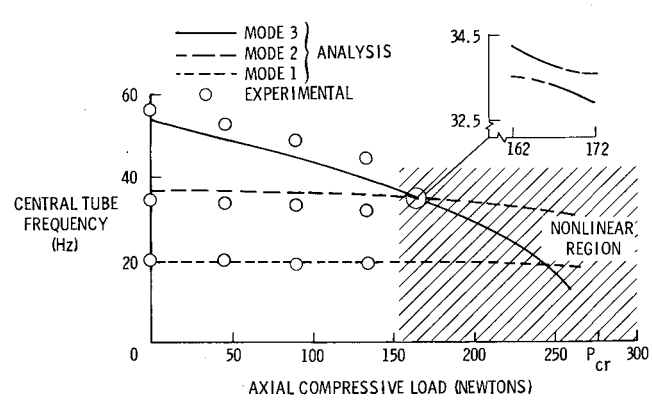

Fig. 13 Effect of compressive load on vibration frequencies.

formed to determine the effects of different stay tension levels on the vibration and buckling characteristics. The tension level in each stay was computed using the design equation from Ref. 5

$$T_n = \frac{8D_n}{9l}\left[4 + (4n^2 + 2)\left(\frac{l}{R}\right)^2\right]\frac{\epsilon P}{1-\lambda} \tag{5}$$

Figure 14 shows the effects of stay tension on central tube natural frequencies. Increasing the stay tension decreases the first three central tube frequencies similarly to applying a compressive end load to the column. However, the lateral stay frequencies increase with increasing tension. By neglecting the bending stiffness of the stays, the equation for lateral frequencies of a taut string

$$f = S(T/\rho)^{\frac{1}{2}}/2L \tag{6}$$

may be used to compute the stay frequency change with changing tension. Equation (6) is a good approximation when the stay ends are relatively fixed and the condition

$$S^2 T_n D_n^2/\pi^2 E_s I_s \gg 1 \tag{7}$$

is satisfied.[11]

Figure 15 shows the effect of stay tension on the buckling load of the column. The induced precompression of the central tube with the increasing stay tension severely lowers the buckling load. This reduced buckling load is the most adverse effect of increasing stay tension.

Experimental verification of stay tension effects was not performed due to spoke buckling at high tension levels and stay slackening at low tension levels. Nevertheless, it is reasonable to have confidence in these trends based on the good agreement between experimental and analytical buckling load and natural frequencies at the design tension level.

Theoretically, to obtain the maximum buckling load, the stay tension level should be as small as the fabrication tolerance permits. However, low tension levels reduce the allowable lateral deflection before occurrence of stay slackening. The possibility of stay slackening creates a small linear range

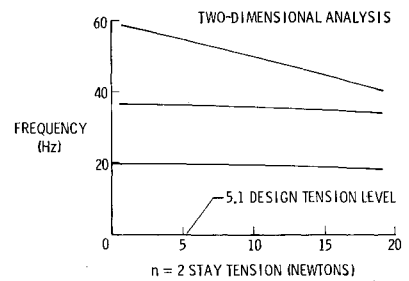

Fig. 14 Effect of stay tension on vibration frequencies.

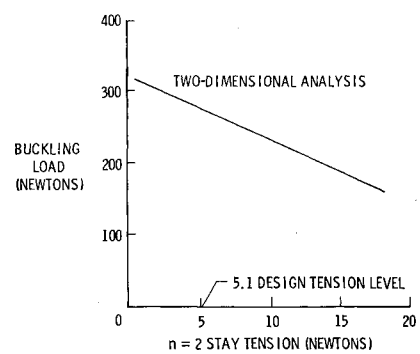

Fig. 15 Effect of stay tension on buckling load.

of lateral deflections and requires nonlinear analysis to be employed at only moderate deflection amplitudes. Thus, a compromise between buckling load and allowable lateral deflections should be evaluated in design when sizing the stay tension level.

Suggested Designer Guidelines

Stay tension levels are perhaps the most difficult aspect of pretensioned structure design. Excessive tension reduces the load-carrying capacity of compression members. On the other hand, insufficient tension could lead to catastrophic failure. The design tension level must consider vibration-load interaction. That is, stay tension levels must be sized to insure that the combined effect of static and dynamic loads is acceptable. This requirement is particularly important since load paths may change significantly if the dynamic environment produces stay slackening.

Physical implementation of tension levels is difficult because of imperfections in member lengths. These imperfections produce tension levels different from those designed. On-orbit adjustment of tension levels appears impractical with present technology; thus, imperfections should be absorbed by passive techniques. One promising technique is the use of buckled struts to pretension members as shown in Fig. 4.

End shortening of compression members at buckling initiates stay slackening and loss of stability. Although the stress of buckling may be low, buckled pretensioned structures may not return to their original shape due to reduced postbuckling restoring forces. A safe margin between operating load and buckling load must be designed if the structure's original shape will not return when the load is removed. Otherwise, buckling may occur and the structure could be salvaged only by redeployment.

Conclusion

Buckling and vibration characteristics of pretensioned structures are investigated through analyses and tests of a stayed column. Finite element analyses are used to show the limits of linear analysis. Nonlinear response due to stay slackening is qualified and several unusual buckling and vibration characteristics are identified.

Correlation between test data and linear analysis is good in the taut stay deflection range of the column. Two-dimensional analysis is as accurate as three-dimensional analysis and reduces computation costs. The initial buckling mode has eight lobes and all stays remain taut until buckling occurs. End shortening which occurs at buckling produces stay slackening, which causes the central tube to buckle in a lower energy mode. Consequently, the postbuckling restoring force is only a fraction ($1/N^2$ in the limit) of the initial buckling load.

High modal density is present near central tube bending modes due to the dimensions and tension levels of the stays. This condition increases the difficulty of reducing test data and could lead to system identification problems if such a structure were to be actively controlled. The frequencies of the first two central tube vibration modes may be raised significantly by increasing the exterior stay extensional stiffness. Compressive loading reduces the third vibration mode frequency more than other modes because the mode shapes of initial buckling and third vibration are identical. Moreover, lateral deflections are amplified by compressive loading and the resulting vibration-load interaction leads to stay slackening, premature buckling, and nonlinear oscillations.

References

[1]Russell, R.A., Cambell, T.G., and Freeland, R.E., "A Technology Development Program for Large Space Antennas," IAF-80 A 33, Sept. 1980.

[2]Howson, W.P. and Williams, F.W., "A Parametric Study of the Initial Buckling of Stayed Columns," *Proceedings of the Institute of Civil Engineers*, Part 2, Vol. 69, June 1980, pp. 261-279.

[3]Heard Jr., W.L., et al., "Structural Sizing Considerations for Large Space Platforms," *Journal of Spacecraft and Rockets*, Vol. 18, Nov.-Dec. 1981, pp. 556-564.
[4]Knapp, K. and Finley, L.A., "Structural Tests on a Self-Expanding Truss Column Model," Astro Research Corp. Carpinteria, California, ARC-TN-1082, Dec. 1979.
[5]Hedgepeth, J.M., "Design of a Self-Expanding Column," Astro Research Corp. Carpinteria, California, ARC-TN-1081, March 1980.
[6]Timoshenko, S., *Theory of Elastic Stability*, 1st ed., McGraw-Hill Book Co., New York, 1936, pp. 100-108.
[7]Williams, F.W. and Howson, W.P., "Concise Buckling Analysis of Stayed Columns," *International Journal of Mechanical Science*, Vol. 20, 1978, pp. 299-313.
[8]Williams, F.W. and Howson, W.P., "Concise Buckling, Vibration and Static Analysis of Structures Which Include Stayed Columns," *International Journal of Mechanical Science*, Vol. 20, 1978, pp. 513-520.
[9]Wittrick, W.H. and Williams, F.W., "Buckling and Vibration of Anisotropic or Isotropic Plate Assemblies Under Combined Loadings," *International Journal of Mechanical Science*, Vol. 16, April 1974, pp. 209-239.
[10]Anderson, M.S., Hennessy, K.W., and Heard, W.L. Jr., "Addendum to Users Guide to VIPASA," NASA TM X0-73914, 1976.
[11]Timoshenko, S., *Vibration Problems in Engineering*, 2nd ed., D. Van Nostrand Co., New York., 1937, pp. 364-368.